Hindawi
Complexity
Volume 2020, Article ID 8820332, 13 pages
https://doi.org/10.1155/2020/8820332

*Research Article*

# Study on Multiobjective Modeling and Optimization of Offshore Micro Integrated Energy System considering Uncertainty of Load and Wind Power

**Jun Wu**,[1] **Baolin Li**,[1] **Jun Chen**,[2] **Qinghui Lou**,[2] **Xiangyu Xing**,[1] **and Xuedong Zhu**[1]

[1]*School of Electrical Engineering & Automation, Wuhan University, Wuhan, China*
[2]*Research Institute Nanjing NARI-Relays Engineering Technology Co., Ltd., Nanjing, China*

Correspondence should be addressed to Baolin Li; baolin-li@whu.edu.cn

Received 21 August 2020; Revised 23 November 2020; Accepted 8 December 2020; Published 24 December 2020

Academic Editor: Xin Li



Offshore micro integrated energy systems (OMIESs) are the basis of offshore oil and gas engineering and play an important role in developing and utilizing marine resources. By introducing offshore wind power generation, the carbon emissions of offshore micro integrated energy systems can be effectively reduced; however, greater challenges have been posted to the reliable operation due to the uncertainty. To reduce the influence brought by the uncertainty, a multiobjective optimization model was proposed based on the chance-constrained programming (CCP); the operating cost and penalty cost of natural gas emission were selected as objectives. Then, the improved hybrid constraints handling strategy based on nondominated sorting genetic algorithm II (IHCHS-NSGAII) was introduced to solve the model efficiently. Finally, the numerical studies verified the efficiency of the proposed algorithm, as well as the validity and feasibility of the proposed model in improving the economy of OMIES under uncertainty.

## 1. Introduction

Currently, there are 6500 offshore oil and gas platforms worldwide [1], which is expected to become an important way to solve energy and environmental problems worldwide by developing and utilizing marine oil and gas resources [2–4]. These offshore oil and gas platforms are far away from the land and can be categorized as an offshore micro integrated energy system [5]. It contains a variety of energy, such as electricity, gas, and heat, and coordinates and optimizes the economy and energy utilization efficiency through energy coupling equipment (such as the power to gas (*P*2*G*) and direct-fired boilers (GB)). Traditionally, that power is provided by gas turbines (GTs) coupled to electric generators, installed on the platforms, and operating by combustion of natural gas; however, for safety considerations, redundant GTs generally run with lower operating efficiency and higher pollution emissions [6, 7]. By introducing offshore wind power, the carbon emissions of offshore micro integrated energy systems (OMIESs) can be effectively reduced. However, affected by the complex offshore environment, greater challenges have been posted to the reliable operation due to the uncertainty of load and offshore wind power [8]. Therefore, it is of great significance to carry out economic optimization dispatch considering the uncertain factors in the OMIES.

At present, scholars have conducted many studies on the optimal operation model of the IES (integrated energy system) [9–12]. In [9], the photovoltaic uncertainty was described by a series of scenarios; then, the model was proposed based on demand response to realizing coordinated optimization for the multiple energy systems. In [10], the modeling of all equipment in the IES was presented to specify the physical operational constraints, and an optimization model was set up to minimize the total cost, considering the heat energy with different grades. Reference [11] studied the influence on the operational costs and the stability of the regional IES when the controllable loads

including electric vehicles and air conditioning loads were considered a virtual energy storage system (ESS). Reference [12] proposed a two-stage stochastic scheduling scheme of an integrated multienergy system, which considers the wind power uncertainty to achieve the optimal economic operation with the minimum curtailment of wind power. The literature listed above proposed different models of IES optimization scheduling, taking into consideration the intermittency of renewable energy, the different grades of heat energy, and the flexibility brought by ESS. However, few of them focus on the optimization of offshore oil and gas platforms and combine the OMIES with offshore wind power as well as considering the effect of uncertainty.

Generally, there are mainly three different ways to handle the uncertainty of offshore wind power, namely, robust optimization [13, 14], interval optimization [15], and stochastic optimization [16, 17]. Among them, stochastic optimal scheduling uses more accurate probability distribution information of uncertain variables to participate in the modeling and solving of scheduling models. The chance-constrained programming (CCP) model allows some constraints containing uncertain variables to fail in the optimization process, but the probability level of its establishment must meet the confidence level requirements. Reference [18] explored the low-carbon and economic planning of OMIES considering the effect of the production process or the uncertainty of the external environment. With the development of offshore wind power, it is necessary to study the economic operation of the system under uncertainty.

In this paper, the improved hybrid constraints handling strategy based on nondominated sorting genetic algorithm II (IHCHS-NSGAII) was introduced to solve the biobjective optimization model based on CCP to minimize the operating cost and natural gas emission. The paper mainly has the following contributions:

(i) A biobjective optimization model based on CCP was proposed to handle the uncertainty of load and wind power. To maximize wind power penetration, the wind curtailment penalty item was added to the cost objective function. Besides, the natural gas emission was selected as the other objective considering the current situation that there exists a large amount of natural gas emission in actual OMIES

(ii) Based on NSGAII, the hybrid constraints handling strategy was introduced and modified through three aspects, namely, dimensionality reduction, individual repair, and normalization to improve the performance of NSGAII when dealing with complex constraints

(iii) The relationship between natural gas emission and wind power utilization was analyzed by implementing an OMIES example in the Bohai Sea to provide schemes or suggestions for offshore oil and gas platforms

The rest of this paper is organized as follows. Section 2 introduces the OMIES. Section 3 formulates the CCP biobjective optimization problem. Section 4 presents IHCHS-NSGAII. Section 5 shows the numerical results and analysis and the conclusion is drawn in Section 6.

## 2. Introduction of OMIES

The energy flow of OMIES is shown in Figure 1, which mainly includes electricity, gas, and thermal. Also, different energy is coupled with conversion equipment; for instance, the GTs burn the exploited natural gas to supply electricity to the entire system and simultaneously utilize the high-temperature flue gas generated by the combustion to heat the system [19]. OMIES is formed by multiple offshore oil and gas center platforms interconnected by submarine cables and transmission pipelines.

Generally, the OMIES is different from a general IES. First of all, for the limitation of the capacity of the offshore platform, energy equipment is placed relatively concentrated on the offshore platforms; the physical distance between "source" and "load" is relatively short. Also, the transmission network is not as complicated as that of a land-based power system. Secondly, ensuring steady and safe production is the most thing for offshore oil and gas engineering, thus leading to the redundant configuration of GTs. Besides, the exploited natural gas that cannot be transmitted will be burned by the torch on the platform due to the limitation of the pipelines' transmission capacity, which is known as natural gas emission. So, it is necessary to do some research based on the characteristics of OMIES.

## 3. CCP Optimization Model

Challenges have been posted to the operation of OMIES due to the uncertainty of load and offshore wind power: on the one hand, in order to reduce pollution emissions and energy waste, the staff hope to reduce the output of GTs and utilize as much wind power as possible; on the other hand, to tackle uncertainty and ensure the safe and stable operation of the system, the power system needs to reserve a certain amount of spare capacity to try to avoid production shutdown due to load shedding, but it will also increase the operating cost of the system. Therefore, it is necessary to establish a multi-objective operation optimization model that takes into account system operating costs and the consumption of wind power.

### 3.1. Objective Functions

*3.1.1. Objective Function 1.* Five parts are included in the operating cost, namely, the pollution cost of GTs and GBs, the cost of gas well production, the penalty cost of natural gas emission, and wind curtailment.

$$\min F_1 = \sum_{t=1}^{T} \left[ \begin{array}{l} \sum_{i\in\Omega_{gt}} \left[ \alpha_{1,i}^{gt} + \alpha_{2,i}^{gt} P_{i,t}^{gt} + \alpha_{3,i}^{gt} \left( P_{i,t}^{gt} \right)^2 \right] + \sum_{j\in\Omega_{gb}} \alpha_j^{gb} G_{j,t}^{gb} \\ + \sum_{k\in\Omega_{cp}} \alpha_k^{\text{well}} G_{k,t}^{\text{well}} + \sum_{k\in\Omega_{cp}} \alpha_k^{\text{gas}} \Delta G_{k,t}^{\text{gas}} + \sum \alpha_i^{\text{wind}} \Delta P_{i,t}^{W} \end{array} \right]. \tag{1}$$

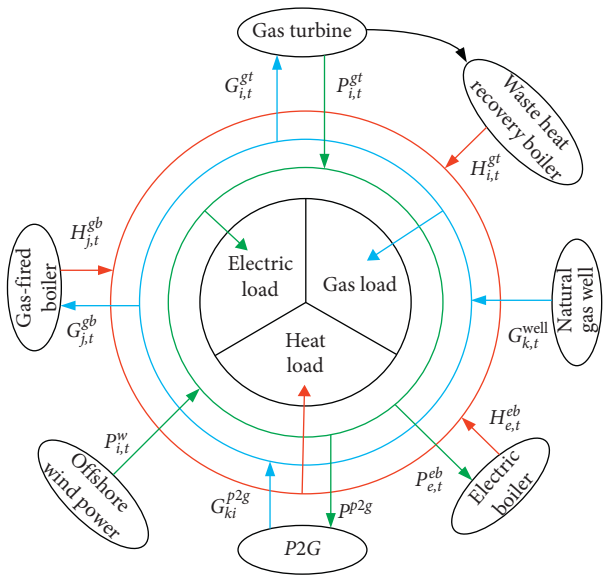


Figure 1: Energy flow of OMIES.

*3.1.2. Objective Function 2.* The natural gas emission not only causes energy waste but also pollutes the environment, so objective function 2 aims to minimize the natural gas emission.

$$\min F_2 = \sum_{t=1}^{T} \sum \Delta G_{k,i}^{\text{gas}}. \tag{2}$$

*3.2. Operation Constraints.* The OMIESs contain various kinds of energy and equipment, and the following four types of constraints shall be met for safe operation.

*3.2.1. Decision Variable Constraints.* Generally, the solution for a practical optimal scheduling problem includes the outputs of all kinds of devices in the whole system, so that the operators can make adjustments at appropriate times to achieve goals. In the OMIES scheduling problem proposed in this paper, the decision variable constraints can be expressed as follows:

$$P_i^{gt,\min} \le P_{i,t}^{gt} \le P_i^{gt,\max}, \tag{3}$$

$$0 \le P_{i,t}^{W} \le P_{i,t}^{W,\text{pre}}, \tag{4}$$

$$G_k^{\text{well, min}} \le G_{k,t}^{\text{well}} \le G_k^{\text{well, max}}, \tag{5}$$

$$0 \le H_{j,t}^{gb} \le H_j^{gb,\max}, \tag{6}$$

$$0 \le H_{e,t}^{eb} \le H_e^{eb,\max}, \tag{7}$$

$$0 \le G_{P2G}^{t} \le G_{P2G}^{t,\max}, \tag{8}$$

$$-\frac{\pi}{2} \le \theta_{h,t} \le \frac{\pi}{2}, \tag{9}$$

$$p_n^{\min} \le p_{n,t} \le p_n^{\max}, \tag{10}$$

$$-R_i^{\text{down}} \le P_{i,t}^{gt} - P_{i,t-1}^{gt} \le R_i^{\text{up}}. \tag{11}$$

Equations (3)–(8) describe the upper and lower bounds of GTs, offshore wind power, gas well, GBs, EBs, and *P2G*, respectively. Equations (9) and (10) are the node angel and node pressure limits. Equation (11) describes the ramp limits of GTs.

*3.2.2. System Balance Constraints.* For each system, the energy flow in and out at each bus shall be equal.

$$\sum_{i\in h} P_{i,t}^{gt} + \sum_{i\in WG} P_{i,t}^{w} - \sum_{g\in h} P_{gh,t} - E_{h,t}^{\text{load}} - \sum_{e\in h} P_{e,t}^{eb} - P^{p2g} = 0, \tag{12}$$

$$\sum_{k\in n} G_{k,t}^{\text{well}} + G_{k,t}^{p2g} + \sum_{m\in n} G_{mn,t} - \sum_{i\in n} G_{i,t}^{gt} - G_{n,t}^{\text{load}} - \sum_{j\in n} G_{j,t}^{gb} - \sum_{k\in n} \Delta G_{k,t}^{\text{gas}} = 0, \tag{13}$$

$$\sum_{i\in\Omega_{gt}} H_{i,t}^{gt} + \sum_{j\in\Omega_{gb}} H_{j,t}^{gb} + \sum_{e\in\Omega_{eb}} H_{e,t}^{eb} - H_t^{\text{load}} = 0. \tag{14}$$

*3.2.3. Equipment Operation Constraints.* Equipment in the OMIES is constrained by energy conservation constraints.

$$P_{i,t}^{W,\text{pre}} - P_{i,t}^{W} = \Delta P_{i,t}^{W}, \tag{15}$$

$$G_{i,t}^{gt} = \frac{P_{i,t}^{gt}}{\eta \cdot HV_{\text{gas}}}, \tag{16}$$

$$H_{i,t}^{gt} = \frac{P_{i,t}^{gt} \cdot \left(1 - \eta_{gt} - \eta_{l}\right) \cdot \eta_{whb}}{\eta_{gt}}, \tag{17}$$

$$H_{j,t}^{gb} = \eta_{gb} \cdot HV_{\text{gas}} \cdot G_{j,t}^{gb}, \tag{18}$$

$$H_{e,t}^{eb} = \eta_{eb} \cdot P_{e,t}^{eb}, \tag{19}$$

$$G_{P2G}^{t} = \frac{\eta_{P2G} P_{P2G}^{t}}{H_{g}}. \tag{20}$$

Equation (15) describes the relationship between actual wind power and forecasted value. Equations (16)–(20) are the relationships between the input and output of each equipment. The power flow constraints of OMIES can be found in [20]. The relationship between the flow of natural gas flowing through a pipeline and the pressure at both ends of the pipeline can be found in [21].

*3.2.4. Chance Constraints.* Offshore oil and gas platforms face a complex and changeable environment. In this paper, the uncertainty of power load and offshore wind power is modeled by stochastic variables. The forecast error of offshore wind power and power load can be expressed by normal distribution as follows:

$$\begin{aligned} \varepsilon_{wt,t} &\sim N\left(0, \sigma_{wt}\right), \\ \sigma_{wt} &= \rho_{wt,t} P_{wt,t} + \rho_{wt,\text{ins}} P_{wt,\text{ins}}, \\ \varepsilon_{\text{load},t} &\sim N\left(0, \sigma_{\text{load}}\right), \\ \sigma_{\text{load}} &= \rho_{\text{load},t} E_{\text{load},t}. \end{aligned} \tag{21}$$

Therefore, the power balance constraint shall be converted as (22) considering the uncertainty.

$$P_{r}\left\{\sum_{i\in h} P_{i,t}^{gt} + \sum_{i\in WG} P_{i,t}^{w} - \sum_{g\in h} P_{gh,t} - \sum_{e\in h} P_{e,t}^{eb} - P^{p2g} - E_{h,t}^{\text{load}}\right\} \geq \eta_{1}. \tag{22}$$

Equation (22) indicates that the power flow shall be met under a certain confidence coefficient.

To ensure the safe operation of the system and prevent the uncertainty of wind power and load from affecting the power balance, the reserve capacity should meet the up- and down-reserve capacity constraints.

$$P_{r}\left\{\sum_{i=1}^{N}\left(P_{i\max} - P_{i}\right) \geq U_{SR} + w_{u} P_{W}\right\} \geq \eta_{2}, \tag{23}$$

$$P_{r}\left\{\sum_{i=1}^{N}\left(P_{i} - P_{i\min}\right) \geq w_{d}\left(P_{W\max} - P_{W}\right)\right\} \geq \eta_{3}. \tag{24}$$

*3.3. Transformation of Chance Constraints.* Chance constraints in equations (22)–(24) are difficult to handle. And it can be solved by converting into their equivalence type [22].

$$\begin{aligned} &\sum_{i\in h} P_{i,t}^{gt} + \sum_{i\in WG} P_{i,t}^{w} - \sum_{g\in h} P_{gh,t} - \sum_{e\in h} P_{e,t}^{eb} - P^{p2g} \\ &\quad - E_{h,t}^{\text{load}} \geq \inf\left\{K | K = \phi_{1}^{-1}\left(\eta_{1}\right)\right\}, \\ &\frac{1}{w_{u}}\left(\sum_{i=1}^{N}\left(P_{i\max} - P_{i}\right) - U_{SR}\right) - P_{i,t}^{w} \geq \inf\left\{K | K = \phi_{2}^{-1}\left(\eta_{2}\right)\right\}, \\ &\frac{1}{w_{d}}\left(\sum_{i=1}^{N}\left(P_{i} - P_{i\min}\right)\right) - P_{wt,\text{ins}} + P_{i,t}^{w} \geq \inf\left\{K | K = \phi_{3}^{-1}\left(\eta_{3}\right)\right\}. \end{aligned} \tag{25}$$

## 4. IHCHS-NSGAII

Although NSGAII [23] is recognized as one of the most effective ways to deal with such multiconstrained problems, the proposed model in Section 3 is still difficult to solve due to the complexity of the variable vectors and different kinds of constraints, especially when there might be coupling and nonlinearity. Therefore, a high efficient optimization method was needed to handle the complex multiconstrained multiobjective optimization problem. In this section, a hybrid constraint processing strategy (HCHS) [24] is introduced and modified to improve the performance of NSGAII when dealing with complex constraints.

*4.1. Dimensionality Reduction Method.* Generally, the equality constraints, such as electric power and gas balance constraints, are not easy to handle for NSGAII, so it is necessary to transfer equality constraints into inequality ones with their own limitations; in the meantime, the vector dimension can be reduced and the solving efficiency of the algorithm would be improved. Taking the power balance constraint as an example, the specific conversion process is as follows.

Equation (12) can be equivalently converted as

$$P_{i,t}^{gt} = P_{gh,t} + E_{h,t}^{\text{load}} + P_{e,t}^{eb} + P^{p2g} - P_{i,t}^{w}. \tag{26}$$

On the other hand, equation (26) shall be met by constraints described in equation (3). Thereby, the equality constraint is equivalently transformed into an inequality one. And the other equality constraints can be converted in the same way.

*4.2. Repair Process after Generation of a New Individual.* Violation of some constraints that are related to the variables generation process, such as the ramp rate constraints, cannot always be reduced for the individuals. Since the individuals are generated using some heuristic-based stochastic methods in NSGAII, the constraint handling method in [23] cannot reduce the violation of some constraints, such as the

ramp rate constraints and the rated power constraints, related to the variables generation process. Thus, a repair process is needed to convert the infeasible individuals into feasible ones. In this paper, the repair process is utilized to repair the variables corresponding to the active power output of GT, which violates the ramp rate constraints. Since the ramp rate constraint violations appear between the variables with close time intervals, which have strong coupling, it is difficult for the optimization algorithm to reduce them during the evolutionary process. Therefore, it is necessary to "repair" the variables when the population is generated. When a ramp rate constraint is violated, all of the variables $P_{i,t}^{gt}$ in a scheduling period should be repaired from the beginning time interval for the related GT, so that the ramp rate limit and the rated power requirement can be met, simultaneously. It is obvious that the repair process may need much computing resources and time. Besides, considering the proportion of infeasible individuals is dynamic during the whole computation period; the repair probability on the infeasible potential solutions is designed to be updated based on the current stage of the algorithm, as shown as follows:

$$P_{\mathrm{re}}(G_c) = \begin{cases} \left(\dfrac{G_c}{G_s}\right)^2, & G_c \le G_s, \\ 1, & G_c > G_s. \end{cases} \tag{27}$$

It can be seen from equation (27) that the value of $P_{\mathrm{re}}$ is small at the beginning of optimization to accept more potential infeasible individuals so that the diversity of the population can be ensured. And when $G_c$ is large enough, all of the individuals which violate the ramp rate constraint should be repaired. But comparing with the microgrid dispatch problem in [24], the OMIES scheduling problem is more complex and the main target is to find feasible solutions. Therefore, to solve the constrained multiobjective problem of OMIES scheduling in this paper, equation (27) is modified as follows:

$$P_{\mathrm{re}}(G_c) = \begin{cases} \dfrac{G_c}{G_s}, & G_c \le G_s, \\ 1, & G_c > G_s, \end{cases} \tag{28}$$

where $G_s = 0.25G_{\max}$. In this way, the average value of $P_{\mathrm{re}}$ is increased compared with that in equation (27), and most of the individuals in the population can be repaired during the optimization process.

*4.3. Normalization Process in Selection.* Considering the types and amounts of constraints in the proposed model, it is efficient to normalize each of the constraint violation before adding up, and the specific details could be found in [24]. It can be seen from Section 2 that in the proposed OMIES scheduling problem, there are various types of constraints, and different types of constraint violations cannot be compared or added directly. Thus, in this paper, the number of violated constraints of different types is also considered as a factor to evaluate the infeasible level of the individuals. The normalization method is modified in this paper as

$$v_{l,k,\mathrm{norm}} = \frac{1}{n_k}\sum_{i=1}^{n_k}\frac{v_{l,k,i} - v_{k,\min}}{v_{k,\max} - v_{k,\min}}. \tag{29}$$

It can be seen from equation (29) that by introducing $n_k$ the normalization process can be more reasonable and the number of violated constraints can be taken into account in the constraints' handling process. Hence, the algorithm would find potential solutions with a lower sum of normalized violations, and the ones with a lower number of violated constraints are preferred during the evolutionary process. Therefore, the average number of violated constraints in the population would drop rapidly, and the feasible regions can be found efficiently.

## 5. Simulation

In this section, the results of the numerical studies are presented and analyzed, which are conducted based on a modified OMIES located in the Bohai Sea of China in [25] as shown in Figure 2. The optimization models are solved under the MATLAB environment. In addition, a computer with Intel i5-8700 CPU@3.20 GHz and 8 GB memory is used to run the optimization models.

*5.1. Parameters of the OMIES.* This case is composed of a 6-node power system, a 6-node natural gas system, and a thermal system. EBs are located in nodes 1, 4, and 5 in the power system with capacities of 1.2 MW, 0.95 MW, and 1.1 MW, respectively. Parameters related to GTs are listed in Table 1. The natural gas system consists of 3 gas well nodes and 3 gas load nodes. GBs are located in nodes 1 and 2 with maximum thermal powers of 3 MW and 4 MW, respectively. Parameters related to the gas well are listed in Table 2. And the natural gas caloricity is 9.7 kWh/m$^3$. The offshore wind turbine is located in node 5 in the power system with a capacity of 9 MW. And the penalty cost coefficient of offshore wind power is 50 \$/MW. Node 2 in the natural gas system and node 4 in the power system are connected by a *P2G* with a capacity of 0.6 MW. The confidence coefficients are all set to 0.95 in this paper. The other parameters could be found in Table 3. By the way, the data used in this paper are collected from an actual offshore oil and gas engineering, and the parameters mentioned above are obtained by fitting or calculating these data.

The forecast curve of electricity, gas, and heat load was shown in Figure 3.

*5.2. Results and Discussions.* The parameters such as the number of population individuals, mutation rate, and calculation accuracy used in IHCHS-NSGAII are selected referring to [24]. The maximum generation number is set to 20000 generations and the population size is 50.

Besides, in this section, the penalty function method (PFM), constraint domination principle (CDP), and the

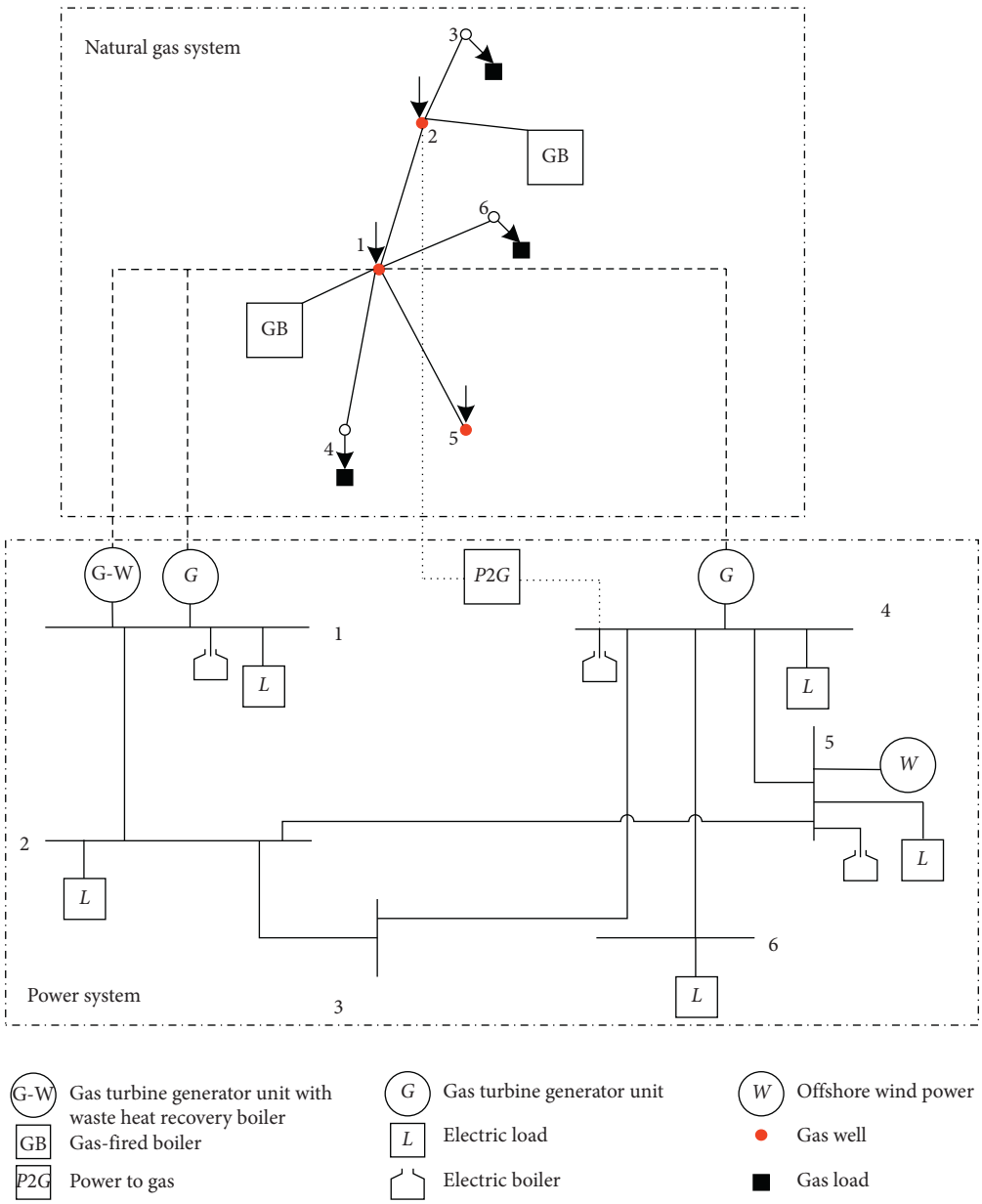


Figure 2: A case of OMIES.

original HCHS are introduced to compare the performance with the improved HCHS. The parameter settings of PFM and HCHS can be found in [24]. Each algorithm is combined with NSGAII and run 10 times. The average feasible solutions using different constraint handling methods are recorded during the evolutionary process.

It can be seen from Table 4 that before 1000 generations, the numbers of feasible solutions obtained are low by all the constraint handling methods, which indicates that the OMIES scheduling problem is very complex with various types of constraints. With the increase of the generations, the feasible solutions become more by CDP, HCHS, and improved HCHS. However, by using PFM, NSGAII cannot find enough feasible solutions. Even after 20000 iterations, NSGAII only finds 15 feasible solutions. As for CDP, the situation is better with 27 solutions, which means that CDP is more effective in dealing with multiconstrained multiobjective optimization problems than PFM. However, nearly half of the obtained solutions are still infeasible. HCHS is based on CDP, but by the hybrid constraints handling methods, it can find more feasible solutions. When HCHS is modified by the method proposed in this paper, it can be seen that it can find a similar amount of feasible solutions with 10000 generations with those by original HCHS after 20000 generations. Moreover, within 18000 iterations, all the solutions in the population are feasible by the proposed improved HCHS. The results indicate that comparing with the existing constraints handling methods, the proposed improved HCHS is more adaptable to the complexity of the multiconstrained OMIES scheduling problem, which can make NSGAII reduce the overall violations considering different constraint types and converge to the feasible

Table 1: Parameters related to GTs [25].

| Number of units | 1 | 2 | 3 |
|---|---|---|---|
| Location of units | 1 | 1 | 4 |
| Maximum output (MW) | 0 | 0 | 0 |
| Minimum output (MW) | 12 | 9 | 12 |
| Maximum ramp up rate (MW/h) | 3 | 2 | 3 |
| Maximum ramp down rate (MW/h) | 3 | 2 | 3 |
| Whether equipped with WHRB | Yes | No | No |
| Quadratic pollution coefficient | 0.0047 | 0.0052 | 0.0074 |
| Linear pollution coefficient | 0.0940 | 0.0730 | 0.1180 |
| Constant coefficient | 0.4900 | 0.2855 | 0.5320 |

Table 2: Parameters related to the gas well.

| Number of gas well | 1 | 2 | 3 |
|---|---|---|---|
| Location of gas well | 1 | 2 | 5 |
| Minimum output of gas well/$10^6$ $m^3$ | 0.1000 | 0.0113 | 0.0050 |
| Maximum output of gas well/$10^6$ $m^3$ | 0.1313 | 0.0158 | 0.0071 |
| Minimum gas emission/$10^6$ $m^3$ | 0 | 0 | 0 |
| Maximum gas emission/$10^6$ $m^3$ | 0.1000 | 0.0113 | 0.0050 |
| Cost coefficients of gas production \$/$10^6$ $m^3$ | 20 | 15 | 25 |
| Penalty cost coefficients of gas emission \$/$10^6$ $m^3$ | 200 | 150 | 250 |

Table 3: Other parameters.

| Parameters | Value |
|---|---|
| Efficiency of GT | 0.4 |
| Heat loss coefficient of GT | 0.3 |
| Heat recovery efficiency of WHRB | 0.47 |
| Combustion efficiency of GB | 0.85 |
| Pollution coefficient of GB | 0.24\$/MW |
| Electrothermal conversion efficiency of EB | 0.99 |
| Reserve capacity factor | 0.12 |
| Error coefficient of offshore wind power capacity | 0.02 |
| Error coefficient of offshore wind power output | 0.2 |
| Error coefficient of power load | 0.2 |

regions faster. Therefore, more computational resources can be applied to find better Pareto solutions.

The optimal solution set is shown in Figure 4.

From the perspective of the distribution of the Pareto set, the operating cost and the natural gas emission cannot be perfectly optimized at the same time. The staff need to weigh environmental protection, economy, and stability according to actual needs. And the final Pareto optimal solution is not continuous. For solutions at discontinuities, one objective function may have a small difference, but the other objective function can be greatly optimized. Therefore, particular attention should be paid to the choice of solutions at discontinuities.

What is more, the optimal solutions in the Pareto set of the two objective functions are selected as the two schemes.

*Scheme One.* The optimal solution for operating cost (operating cost 809.4448 \$ and natural gas emission 400.00 $m^3$).

*Scheme Two.* The *optimal* solution for natural gas emission (operating cost 877.844 \$ and natural gas emission 21.00 $m^3$).

The operating cost comparison of the two schemes is shown in Figure 5, and the specific operating cost values are shown in Table 4.

It can be seen from Figure 5 and Table 5 that the pollution cost of GBs in the two schemes is basically the same. The pollution cost of GTs and GBs, cost of the gas well, and the penalty cost of wind curtailment in scheme one are lower than those in scheme two, while the penalty cost of gas

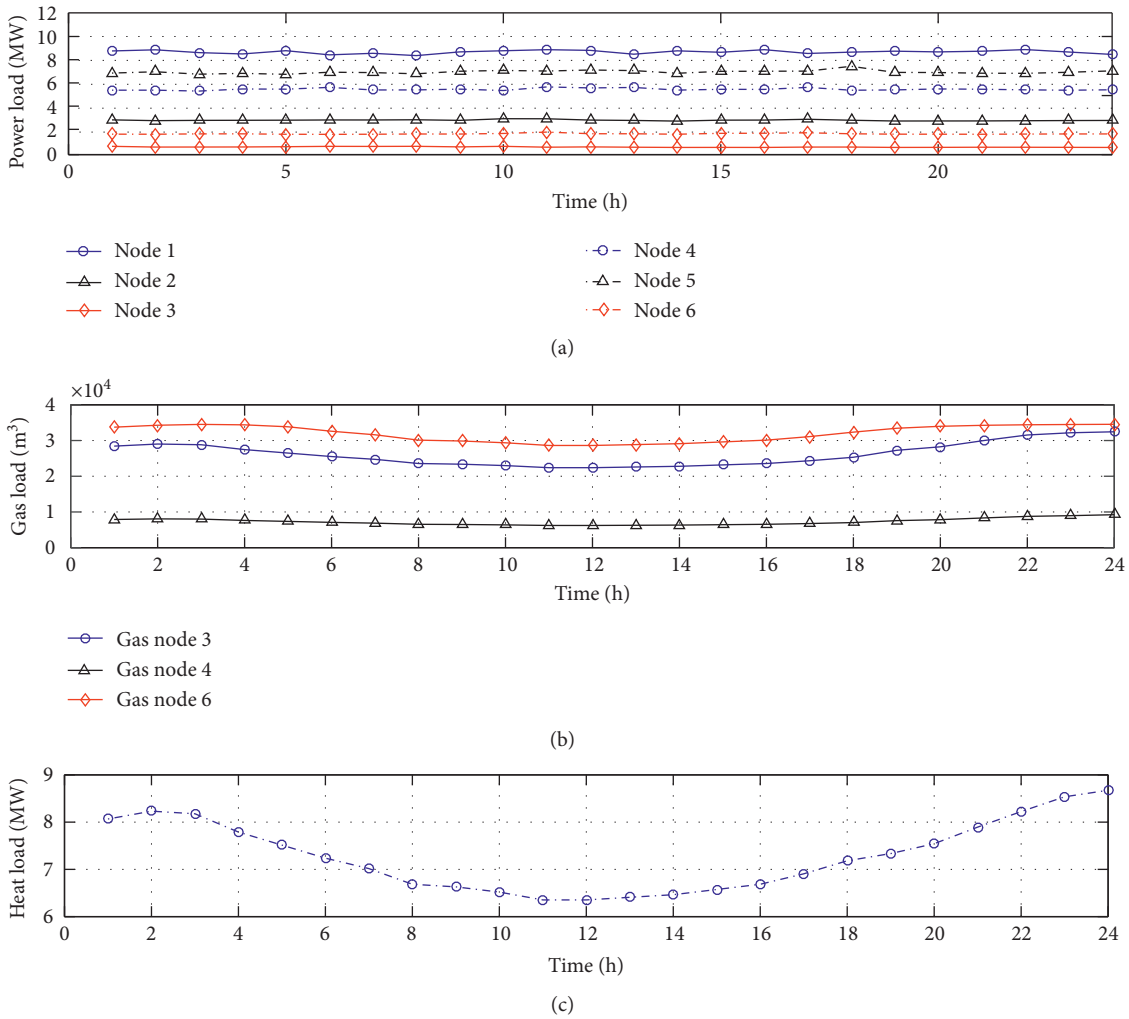


Figure 3: Different load forecast curves.

Table 4: Average feasible solutions using different constraint handling methods during the evolutionary process.

| Generations | 100 | 500 | 1000 | 3000 | 5000 | 10000 | 15000 | 18000 | 20000 |
|---|---|---|---|---|---|---|---|---|---|
| PFM | 0 | 2 | 6 | 5 | 8 | 7 | 11 | 13 | 15 |
| CDP | 0 | 4 | 9 | 13 | 18 | 24 | 27 | 25 | 27 |
| HCHS | 1 | 5 | 11 | 20 | 22 | 29 | 35 | 39 | 38 |
| Improved HCHS | 3 | 7 | 12 | 22 | 27 | 36 | 47 | 50 | 50 |

emission is opposite since the objective functions of the two schemes are different. The operating cost in scheme one is lower than that in scheme two, about 10.5% lower. It can be seen that when more offshore wind power is consumed, operating costs can be effectively reduced in terms of pollution cost and gas production cost; however, this will also increase natural gas emission.

It can be seen from Figures 6 and 7 that in the actual utilization of offshore wind power, scheme one is slightly better than scheme two. Both schemes show that the optimization strategy used in this paper keeps the curtailed offshore wind power at a very low level for most of the scheduling cycle, and the peak of the curtailed power occurs only around 12–15 hours.

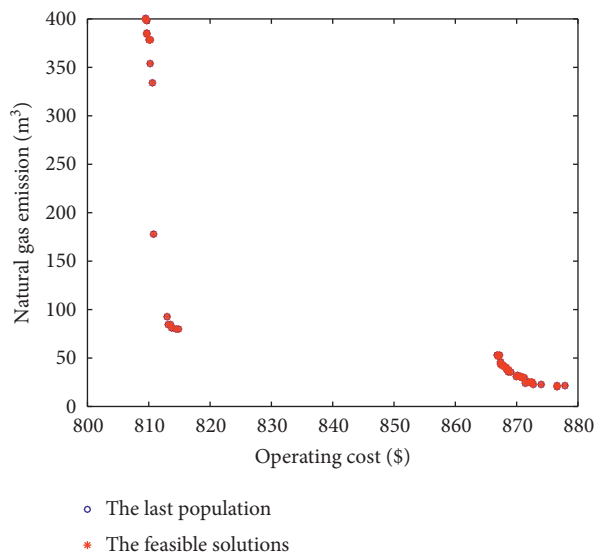


Figure 4: The Pareto set obtained by IHCHS-NSGAII.

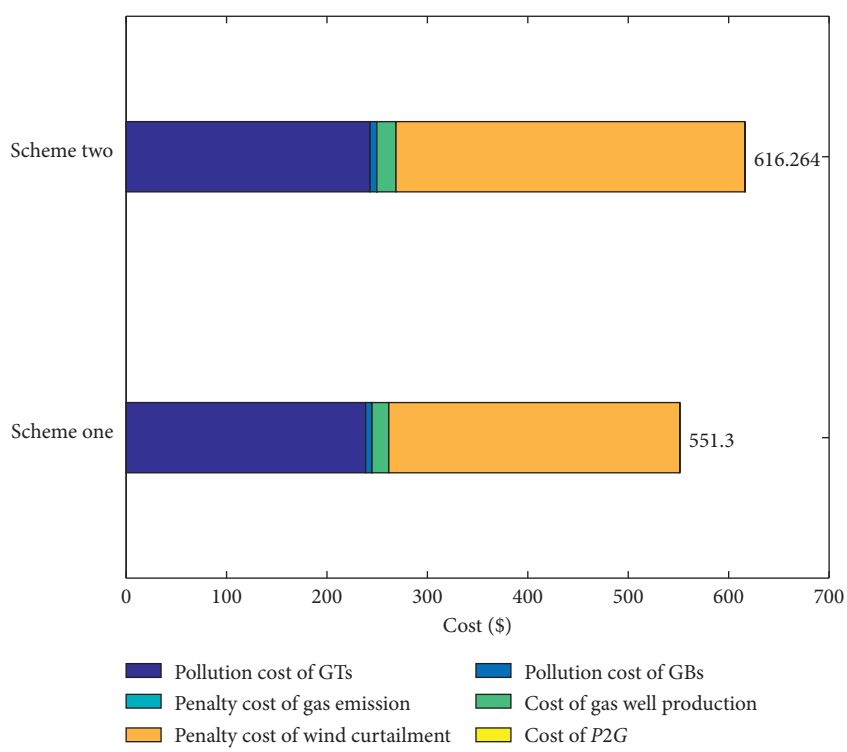


Figure 5: Operating cost structure under different schemes.

Table 5: Specific operating cost values.

| Schemes | Pollution cost of GTs/$ | Pollution cost of GBs/$ | Penalty cost of gas emission/$ | Cost of gas well/$ | Penalty cost of wind curtailment/$ |
|---|---|---|---|---|---|
| One | 238.5283 | 6.3072 | 0.0142 | 16.7387 | 289.7100 |
| Two | 242.9183 | 6.7028 | 0.0008 | 19.1436 | 347.4900 |

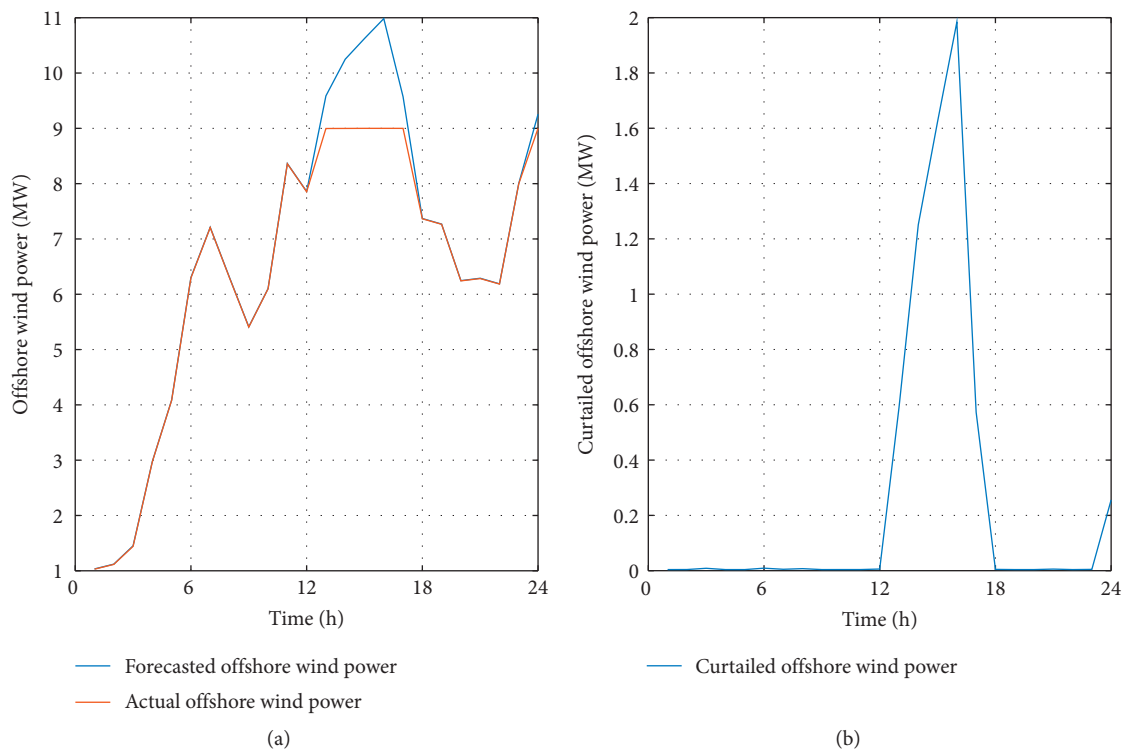


Figure 6: Forecasted and actual offshore wind power in scheme one.

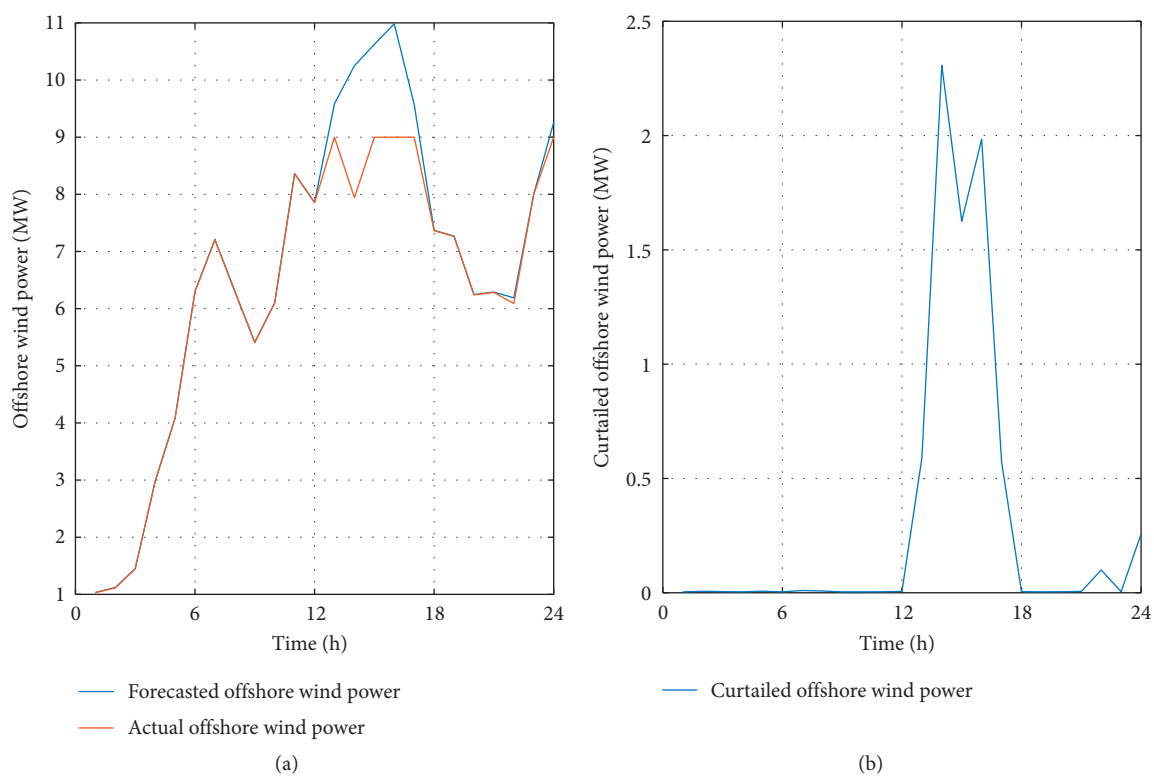


Figure 7: Forecasted and actual offshore wind power in scheme two.

## 6. Conclusion

While offshore wind power reduces environmental pollution, it also has an impact on the safe and stable operation of OMIES. In this paper, a biobjective optimization model based on the CCP was proposed to improve the economy of OMIES and reduce the natural gas emission; therefore, the natural gas emission and the operating cost containing the pollution cost and wind curtailment penalty cost are selected, respectively, as objective functions. Besides, the IHCHS-NSGAII was proposed to solve the multiconstrained biobjective model fast and efficiently from three aspects, namely, dimensionality reduction, individual repair process, and normalization and weighted sum process in selection. Then, it was applied to an OMIES problem, and the results show that the proposed method can make NSGAII converge to the feasible regions faster; thus, more computational resources can be applied to find better Pareto solutions. Besides, the operating cost and the natural gas emission cannot be perfectly optimized at the same time since the Pareto set is discontinuous. Also, the utilization of offshore wind power improves the economy of OMIES but increases natural gas emissions. Further studies are needed on the influence of the energy storage systems such as battery and gas/heat storage facilities.

## Abbreviations

| | |
|---|---|
| OMIES: | Offshore micro integrated energy system |
| IES: | Integrated energy system |
| CCP: | Chance-constrained programming |
| GT: | Gas turbine |
| GB: | Gas-fired boiler |
| EB: | Electric boiler |
| ESS: | Energy storage system |
| NSGA II: | Nondominated sorting genetic algorithm II |
| PFM: | Penalty function method |
| CDP: | Constraint domination principle |
| HCHS-NSGAII: | Hybrid constraints handling strategy NSGAII |
| IHCHS-NSGAII: | The improved hybrid constraints handling strategy based on nondominated sorting genetic algorithm II. |

### *Mathematical Symbols*

| | |
|---|---|
| $t$: | Index for hours |
| $i$: | Index for GTs |
| $j$: | Index for GBs |
| $k$: | Index for central platforms |
| $(g, h)$: | Index for power system nodes |
| $(m, n)$: | Index for gas system nodes |
| $e$: | Index for EBs. |

### *Sets*

| | |
|---|---|
| $\Omega_{gt}$: | Set of GTs |
| $\Omega_{cp}$: | Set of central platforms |
| $\Omega_{gb}$: | Set of GBs |
| $\Omega_{eb}$: | Set of EBs. |

### *Variables*

| | |
|---|---|
| $P_{i,t}^{gt}$: | Active power output of GT $i$ in period $t$ |
| $G_{j,t}^{gb}$: | Gas consumed by GB $j$ in period $t$ |
| $\Delta G_{k,t}^{\text{gas}}$: | Gas emission of central platform $k$ in period $t$ |
| $\theta_{g,t}$: | Voltage angel of the power system at node $g$ in period $t$ |
| $P_{e,t}^{eb}$: | Power consumed by EB $e$ in period $t$ |
| $p_{n,t}$: | Pressure of gas system at node $n$ in period $t$ |
| $G_{k,t}^{\text{well}}$: | Gas generated by gas well $k$ in period $t$ |
| $G_{i,t}^{gt}$: | Gas consumed by GT $i$ in period $t$ |
| $\Delta P_{i,t}^{W}$: | Curtailed offshore wind power in period $t$ |
| $P_{i,t}^{W}$: | Actual offshore wind power in period $t$ |
| $P_{i,t}^{W,\text{pre}}$: | Forecasted offshore wind power in period $t$ |
| $\alpha_i^{\text{wind}}$: | Penalty cost of curtailed offshore wind power |
| $P_i^{gt,\max}, P_i^{gt,\min}$: | Maximum and minimum output of GT $i$ |
| $\alpha_{1,i}^{gt}, \alpha_{2,i}^{gt}, \alpha_{3,i}^{gt}$: | Pollution coefficients of GT $i$ |
| $\alpha_j^{gb}$: | Emission coefficient of GB $j$ |
| $\alpha_k^{\text{well}}$: | Gas production coefficient of central platform $k$ |
| $\alpha_k^{\text{gas}}$: | Gas emission coefficient of central platform $k$ |
| $x_{gh}$: | Reactance of transmission line $(g, h)$ |
| $P_{gh}^{\max}$: | Capacity of transmission line $(g, h)$ |
| $R_i^{\text{up}}, R_i^{\text{down}}$: | Ramp up and ramp down limit of GT $i$ |
| $E_{h,t}^{\text{load}}$: | Power load at node $h$ in period $t$ |
| $C_{mn}$: | Constants related to temperature, length, diameter, friction, etc. of pipe $(m, n)$ |
| $G_k^{\text{well},\max}, G_k^{\text{well},\min}$: | Maximum and minimum production of gas well $k$ |
| $p_n^{\max}, p_n^{\min}$: | Maximum and minimum pressure of node $n$ |
| $G_{n,t}^{\text{load}}$: | Gas load at node $n$ in period $t$ |
| $H_t^{\text{load}}$: | Heat load in period $t$ |
| $H_j^{gb,\max}$: | Maximum output thermal power of GB $j$ |
| $\eta_{gt}$: | Efficiency of GT |
| $\eta_l$: | Thermal loss coefficient of GT |
| $\eta_{whb}$: | Heat recovery efficiency of WHRB |
| $HV_{\text{gas}}$: | Natural gas caloricity |
| $\eta_{eb}$: | Efficiency of EB |
| $P_{gh,t}$: | Power transmitted between line $g$and $h$ in period $t$ |
| $G_{mn,t}$: | Gas transmitted between pipe $m$ and $n$ in period $t$ |
| $H_{i,t}^{gt}$: | Heat power provided by WHRB connected with GT $i$ in period $t$ |
| $H_{j,t}^{gb}$: | Heat power provided by GB $j$ in period $t$ |
| $H_{e,t}^{eb}$: | Heat power provided by EB $k$ in period $t$ |

| | |
|---|---|
| $G_{P2G}^{t}$: | Gas converted by $P2G$ in period $t$ |
| $G_{P2G}^{t,\max}$: | Maximum output of $P2G$ |
| $\eta_{P2G}$: | Conversion efficiency of $P2G$ |
| $\varepsilon_{wt,t}$, $\varepsilon_{\text{load},t}$: | Stochastic variables that describe the forecast error of offshore wind power and power load |
| $\sigma_{wt}$, $\sigma_{\text{load}}$: | Variance of forecast error of offshore wind power and power load |
| $\rho_{wt,t}$, $\rho_{wt,\text{ins}}$: | Error coefficient of offshore wind power output and capacity |
| $\rho_{\text{load},t}$: | Error coefficient of power load |
| $\eta_1$, $\eta_2$, $\eta_3$: | Confidence coefficient of power balance constraint, up-reserve capacity constraint, and down-reserve capacity constraint |
| $U_{SR}$: | Coefficient of the reserve requirement |
| $w_u$, $w_d$: | Offshore wind power output demand coefficient for up- and down-reserve |
| $\phi_1^{-1}(\eta_1)$, $\phi_2^{-1}(\eta_1)$, $\phi_3^{-1}(\eta_1)$: | Inverse function of the normal distribution function |
| $G_c$, $G_s$: | Current and switch generation |
| $P_{\text{re}}$: | Repair probability |
| $v_{k,\min}$, $v_{k,\max}$: | Minimum and maximum violation |
| $v_{l,k,i}$: | $i$-th constraint violation of the $l$-th individual |
| $n_k$: | Number of violated $k$-th type of constraints. |

## Data Availability

The table data and modeling data used to support the finding of this study are included within the article.

## Conflicts of Interest

The authors declare that they have no known competing financial interests or personal relationships that could have appeared to influence the work reported in this paper.

## Acknowledgments

This work was supported by the National Key Research and Development Program of China, China (No. 2018YFB0904800).

## References

[1] M. Leporini, B. Marchetti, F. Corvaro, and F. Polonara, "Reconversion of offshore oil and gas platforms into renewable energy sites production: assessment of different scenarios," *Renewable Energy*, vol. 135, pp. 1121–1132, 2019.

[2] S. D. Musa, T. Zhonghua, A. O. Ibrahim, and M. Habib, "China's energy status: a critical look at fossils and renewable options," *Renewable and Sustainable Energy Reviews*, vol. 81, pp. 2281–2290, 2018.

[3] Maribus gGmbH, *The World Ocean Review-Marine Resources Opportunities and Risks*, Maribus Gemeinnützige GmbH, Hamburg, Germany, https://worldoceanreview.com/wp-content/downloads/wor3/WOR3_en.pdf.

[4] S. Van Elden, J. Meeuwig, J. M. Hemmi, and R. Hobbs, "Offshore oil and gas platforms as novel ecosystems: a global perspective," *Frontiers in Marine Science*, vol. 6, p. 548, 2019.

[5] A. Zhang, G. Peng, W. Yang, G. Qu, and H. Huang, "Risk assessment of offshore micro integrated energy system based on fluid mosaic model," *IEEE Access*, vol. 8, pp. 76715–76725, 2020.

[6] W. He, K. Uhlen, M. Hadiya, Z. Chen, G. Shi, and E. del Rio, "Case study of integrating an offshore wind farm with offshore oil and gas platforms and with an onshore electrical grid," *Journal of Renewable Energy*, vol. 2013, Article ID 607165, 10 pages, 2013.

[7] S. Oliveira-Pinto, P. Rosa-Santos, and F. Taveira-Pinto, "Electricity supply to offshore oil and gas platforms from renewable ocean wave energy: overview and case study analysis," *Energy Conversion and Management*, vol. 186, pp. 556–569, 2019.

[8] M. L. Kolstad, A. R. Årdal, K. Sharifabadi, and T. M. Undeland, "Integrating offshore wind power and multiple oil and gas platforms to the onshore power grid using VSC-HVDC technology," *Marine Technology Society Journal*, vol. 48, no. 2, pp. 31–44, 2014.

[9] J. Zhai, X. Wu, S. Zhu, B. Yang, and H. Liu, "Optimization of integrated energy system considering photovoltaic uncertainty and multi-energy network," *IEEE Access*, vol. 8, pp. 141558–141568, 2020.

[10] J. Zheng, Y. Kou, M. Li, and Q. Wu, "Stochastic optimization of cost-risk for integrated energy system considering wind and solar power correlated," *Journal of Modern Power Systems and Clean Energy*, vol. 7, no. 6, pp. 1472–1483, 2019.

[11] L. Bigarelli, A. Lidozzi, M. Di Benedetto, L. Solero, and S. Bifaretti, "Model predictive energy management for sustainable off-shore oil and gas platforms," in *Proceedings of the 2019 21st European Conference on Power Electronics and Applications (EPE'19 ECCE Europe)*, Genova, Italy, September 2019.

[12] A. Turk, Q. Wu, M. Zhang, and J. Østergaard, "Day-ahead stochastic scheduling of integrated multi-energy system for flexibility synergy and uncertainty balancing," *Energy*, vol. 196, pp. 117–130, 2020.

[13] C. Zhao, J. Wang, J.-P. Watson, and Y. Guan, "Multi-stage robust unit commitment considering wind and demand response uncertainties," *IEEE Transactions on Power Systems*, vol. 28, no. 3, pp. 2708–2717, 2013.

[14] R. Jiang, J. Wang, and Y. Guan, "Robust unit commitment with wind power and pumped storage hydro," *IEEE Transactions on Power Systems*, vol. 27, no. 2, pp. 800–810, 2011.

[15] H. Pandžić, Y. Dvorkin, T. Qiu, Y. Wang, and D. S. Kirschen, "Toward cost-efficient and reliable unit commitment under uncertainty," *IEEE Transactions on Power Systems*, vol. 31, no. 2, pp. 970–982, 2015.

[16] H. Wu, M. Shahidehpour, Z. Li, and W. Tian, "Chance-constrained day-ahead scheduling in stochastic power system operation," *IEEE Transactions on Power Systems*, vol. 29, no. 4, pp. 1583–1591, 2014.

[17] Q. Wang, Y. Guan, and J. Wang, "A chance-constrained two-stage stochastic program for unit commitment with uncertain wind power output," *IEEE Transactions on Power Systems*, vol. 27, no. 1, pp. 206–215, 2011.

[18] A. Zhang, H. Zhang, J. Wu, M. Qadrdan, and Q. Li, "Multi-objective stochastic planning for offshore micro integrated energy systems," *Automation of Electric Power Systems*, vol. 43, no. 7, pp. 129–135, 2019.

[19] D. V. Singh and E. Pedersen, "A review of waste heat recovery technologies for maritime applications," *Energy Conversion and Management*, vol. 111, pp. 315–328, 2016.

[20] D. Sun, X. Xie, J. Wang, Q. Li, and C. Wei, "Integrated generation-transmission expansion planning for offshore oilfield power systems based on genetic Tabu hybrid algorithm," *Journal of Modern Power Systems and Clean Energy*, vol. 5, no. 1, pp. 117–125, 2017.

[21] C. M. Correa-Posada and P. Sánchez-Martín, "Integrated power and natural gas model for energy adequacy in short-term operation," *IEEE Transactions on Power Systems*, vol. 30, no. 6, pp. 3347–3355, 2014.

[22] J. Wu, B. Zhang, Y. Jiang, P. Bie, and H. Li, "Chance-constrained stochastic congestion management of power systems considering uncertainty of wind power and demand side response," *International Journal of Electrical Power & Energy Systems*, vol. 107, pp. 703–714, 2019.

[23] K. Deb, A. Pratap, S. Agarwal, and T. Meyarivan, "A fast and elitist multiobjective genetic algorithm: NSGA-II," *IEEE Transactions on Evolutionary Computation*, vol. 6, no. 2, pp. 182–197, 2002.

[24] X. Li, J. Lai, and R. Tang, "A hybrid constraints handling strategy for multiconstrained multiobjective optimization problem of microgrid economical/environmental dispatch," *Complexity*, vol. 2017, Article ID 6249432, 12 pages, 2017.

[25] J. Wu, B. Li, J. Chen et al., "Multi-objective optimal scheduling of offshore micro integrated energy system considering natural gas emission," *International Journal of Electrical Power & Energy Systems*, vol. 125, Article ID 106535, 2021.